Preserved Nd-Hf-Os isotope variability in replacive channels reveals incomplete melt aggregation in the shallow mantle

A. Sanfilippo,[1,2*] C.Z. Liu,[3] V. Salters,[4] A. Mosconi,[5] A. Zanetti,[2] & R. Tribuzio[1,2,6]

[1]Dipartimento di Scienze della Terra e dell'Ambiente, Università degli Studi di Pavia, via Ferrata 1, Pavia, Italy
[2]Istituto Geoscienze e Georisorse, Consiglio Nazionale delle Ricerche, Via Ferrata 1, Pavia, Italy
[3] State of Key Laboratory of Lithospheric Evolution, Institute of Geology and Geophysics, Chinese Academy of Sciences, Beijing, China
[4]Department of Earth, Ocean and Atmospheric Science and National High Magnetic Field Laboratory, Florida State University, Tallahassee, Florida, USA
[5]Department of Earth Sciences "A. Desio", Università degli Studi di Milano, Via Botticelli 23, 21133 Milan, Italy
[6]Istituto Nazionale di Oceanografia e di Geofisica Sperimentale, Borgo Grotta Gigante 42/C, 34010 Sgonico, Trieste, Italy

Abstract

Long-lived radiogenic isotopes of abyssal peridotites, residues of MORB extraction, show that the asthenosphere is intrinsically heterogeneous, which is inherited from ancient melting events and crustal recycling during Earth's history. Yet, MORB have a rather uniform average composition, suggesting that the variability of their mantle source is concealed during their ascent. Here we document that mantle heterogeneity is exceptionally well preserved in high permeability mantle conduits from the Lanzo South mantle massif, Western Italian Alps. Nd-Hf-Os isotopes of decametre-scale replacive bodies provide evidence for the existence of two generations of mantle channels. The first generation consists of dunites concordant to the main foliation of host peridotites. The replacive dunites include clinopyroxene with MORB-like incompatible element signature and initial (160 Ma) ƐNd and ƐHf ranging from +4 to +7 and from +10 to +15, respectively. The second generation, made up of pyroxene-poor harzburgites discordant to the main foliation, is geochemically depleted in incompatible elements and its clinopyroxene displays highly radiogenic Hf isotopes (initial ƐHf up to +202). The mantle channel heterogeneity is confirmed by Re-Os isotopes and platinum-groups elements. The MORB-type dunites have high Pt, Pd and, locally, Re, and have high $^{187}Os/^{188}Os$ ratios (0.122-0.128). On the other hand, the depleted bodies have lower Pt, Pd and Re, and $^{187}Os/^{188}Os$ ratios ranging from those of host peridotites (0.124) to highly unradiogenic values (0.118). The preserved heterogeneity in trace elements, PGE, and Nd-Hf-Os isotopes highlights infiltration of melts from produced by a highly heterogeneous mantle. By consequence, this study demonstrates that the isotopic variability of melts migrating through the shallow mantle is by far larger than magmas erupted on the seafloor, which implies that diverse mantle components are delivered and homogenized above the crust-mantle boundary.

Keywords: *Re-Os isotopes; replacive mantle dunites; Alpine Ophiolites; melt-rock reaction; mantle melting*

1. Introduction

Erupted along the global mid-ocean ridges, MORB (mid-ocean ridge basalts) are the most abundant magmas on Earth, produced by decompression of the asthenosphere in a melting region some hundreds of kilometres wide. To be erupted along the spreading axis, mantle melts must be coalesced from an extremely large area into a narrow zone few kilometres wide (McKenzie et al., 1984). During transport from the source region, MORB can experience magma mixing, crystal fractionation and reaction between migrating magmas and the surrounding mantle, which can influence fundamentally the major, trace elements and isotopic records of the primary mantle melts and thus might conceal the original compositional variabilities in their mantle sources (Grove et al., 1992; Langmuir et al., 1992; Stracke et al., 2012; Wanless and Shaw, 2012; Rudge et al., 2013; Liu and Liang, 2017; Sanfilippo et al., 2021). In addition, retrieving information on the compositional variability of the MORB source is further complicated by the heterogeneity of the mantle before entering the melting region. Such a heterogeneity is mainly documented by the extent of radiogenic isotope variability (i.e., Sm-Nd, Lu-Hf and Re-Os) of abyssal peridotites compared to erupted MORB (Snow et al., 1994; Salters and Dick, 2002; Cipriani et al., 2004; 2010; Harvey et al., 2006; 2011; Liu et al., 2008; 2022; Warren et al., 2009; Stracke et al., 2011; Mallick et al., 2014; 2015; Lassiter et al., 2014; Day et al., 2017; Sani et al., 2023), which implies the preservation of km-scale mantle parcels with different histories of melt depletion and/or chemical enrichments. Hence, erupted basalts cannot be used as direct proxies of their source materials, being biased towards the composition of the most fertile (i.e., fusible) components (Stracke and Burton, 2009; Salters et al., 2011; Stracke, 2012; Rudge et al., 2013; Sanfilippo et al., 2019; 2021). As our knowledge of the chemical heterogeneity of the mantle increases, the mechanism, style and depth of melt aggregation are some of the most challenging issues to decipher (Lambart et al., 2019).

Studies of ophiolites provided the evidence that melt transport mainly occurs within high porosity channels, isolated from the host pyroxene-bearing peridotites by pyroxene-poor walls (Aharonov et al., 1995; Kelemen et al., 1995; Spiegelman et al., 2001). These olivine-rich lithologies form as result of disequilibrium between the basaltic melt and the host pyroxene-bearing peridotites and are often referred to as replacive dunites (Quick, 1981). Experimental and theoretical studies confirm that these dunites represent permeability barriers and prevent further interactions between melts and shallow peridotites (Morgan and Liang, 2005; Liang and Parmentier, 2010; Liang et al., 2011). An interconnected network of highly permeable dunite channels may thereby allow basaltic melts to efficiently segregate from their source region (Kelemen et al., 1997; Spiegelman and Kelemen, 2003; Akizawa et al., 2016). However, to what extent replacive mantle channels can preserve the chemical variability of the migrating melts is still a matter of debate (see Morishita et al., 2011; Tamura et al., 2016; Sanfilippo et al., 2017; Xiong et al., 2022).

In this study, we combined the Nd-Hf isotopic compositions of clinopyroxene and whole-rock Os isotopes of several decameter-scale replacive bodies from the Jurassic Lanzo ophiolite (Western Italian Alps) to explore the extent of variability of melts delivered from the mantle towards the lower crust. We revealed the existence of two generations of large-scale replacive bodies, formed by melts having markedly different trace elements and Nd-Hf-Os isotope signatures. On this basis, we inferred that the fingerprint of a heterogeneous mantle is preserved in mantle migration channels and that diverse mantle components must be delivered and homogenized within lower crustal reservoirs.

2. The Jurassic Lanzo ophiolite

The Lanzo peridotite massif is located in the Western Alps, between the continental units of the Sesia-Lanzo zone and the meta-ophiolites units from the Jurassic Ligurian-Piedmontese basin (Fig. 1). A large proportion of the ultramafic massif is formed by fresh peridotites, consisting of spinel-plagioclase lherzolites/harzburgites, dunites and rare pyroxenites (Boudier, 1978; Bodinier, 1988; Müntener et al., 2005; Piccardo et al., 2007). This mantle sequence is locally intruded by Middle Jurassic MORB-type gabbros (Kaczmarek et al., 2008). Based on the geochemical and geochronological characteristics of these gabbroic and basaltic dykes (Bodinier et al., 1986; Rubatto et al., 2008), and the compositional similarity of the Jurassic sedimentary cover with those of other Jurassic ophiolite sections in the Alps and Apennines (Lagabrielle et al., 1989), there is a general consensus that the Lanzo Massif represents an ophiolitic mantle section exposed at the seafloor in the Jurassic (e.g., Müntener et al., 2005; Piccardo et al., 2007; Kaczmarek and Müntener, 2010; Sanfilippo et al., 2014; 2017; McCharty and Müntener, 2019; McCharty et al., 2021).

Major, trace elements and isotopic compositions of the peridotites allow the Lanzo ultramafic massif to be subdivided three domains, namely South, Central and North (Fig. 1). These domains are physically separated by pre-Alpine mylonitic shear zones, and display distinct geochemical characteristics (Boudier and Nicolas, 1977) (Fig. 1a). The peridotites from the Northern and the Central bodies have fertile chemical compositions and highly depleted Nd isotopic ratios, whereas the peridotites from the Southern body are more refractory and display a Nd isotopic signature similar to MORB (Bodinier et al., 1991). Based on these data, Bodinier et al. (1991) interpreted the Northern and Central portion of the massif as fragments of the sub-continental lithosphere, and the Lanzo South domain as an asthenospheric diapir emplaced during the opening of the Ligurian-Piemontese basin.

These ideas have been reviewed by new concepts developed to explain the similarity of most ophiolitic sections exposed in the Alps and Apennine with the lithosphere formed in hyper-extended magma-poor rifted margins (Müntener and Manatschal, 2006). In particular, the Lanzo South peridotites were proposed to have been formed by a complex history of interaction between a depleted spinel-facies mantle protolith and migrating MORB-type melts produced by asthenospheric upwelling in conjunction with the opening of the Jurassic basin (Müntener et al., 2005; Piccardo et al., 2007) (Fig. 1b). These peridotites typically show crystallization of magmatic plagioclase (Pl) and/or pyroxene within the pre-existing peridotite minerals. These minerals were interpreted to have formed by a melt-peridotite reaction that led to a chemical refertilization of the peridotite, thereby erasing the original geochemical signature of the spinel-facies mantle protolith (see also Müntener et al., 2010). For instance, the spinel in the Pl-peridotites has high Cr#, TiO_2 and MgO, resulting from melt-peridotite reaction (Dick and Bullen, 1984). The incompatible trace element compositions of clinopyroxene (Piccardo et al., 2007) and olivine (Sanfilippo et al., 2014) in the Pl-peridotites indicate that the interacting melts had a MORB-like geochemical signature (see also Sanfilippo et al., 2014). The melt-peridotite reaction event forming the Pl-peridotites was followed by the formation of replacive mantle dunites and, lately, by the intrusion of MORB-like gabbro dykelets and dykes showing diffuse to sharp contacts with respect to the host rocks. U-Pb ages of zircons in oxide-gabbros yield 158 to 163 Ma ages, constraining the age of the migration event (Kaczmarek, et al., 2008). Hence, it is now thought that the Lanzo South sequence represents a fertilised lithospheric domains, intruded and modified by interactions with MORB-like melts during opening of an embryonic oceanic basins akin to the Atlantic or Indian oceans (see Picazo et al., 2016 for a review).

3. Compositional heterogeneity of the Lanzo South replacive bodies

Large replacive bodies are characteristic of the Southern portion of the massif, where they occur in channel-like bodies up to tens of meter in scale (Fig. 1b). Replacive rocks range in composition from pyroxene-free dunites (Fig. 2) to pyroxene-poor harzburgites (Fig. 3), which are concordant and discordant to the main foliation, respectively (Piccardo et al., 2007). The two generations of replacive bodies have distinct geochemical compositions, which were related to the migration with melts with different geochemical affinities (see Fig. 4) (Sanfilippo et al., 2014; 2017; 2019). The concordant dunites have high Fo olivine (89-90) characterized by minor and trace element compositions similar to MORB phenocrysts. Despite this, olivine (Ol) in some of the selected dunites bodies have anomalously high H contents (15-30 ppm), and high Ti/Li and Ti/Sc ratios, likely related to high contributions of geochemical enriched lithologies (Fig. 4b). This agrees with the transitional MORB-like incompatible trace elements of the clinopyroxene (Cpx) locally found as interstitial grain or veinlets within the dunite matrix, which is locally enriched in LILE and LREE compared to N-MORB (see also Müntener et al., 2005; Piccardo et al., 2007) (Fig. 4c).

Conversely, decameter-scale discordant replacive bodies are constituted by chemically depleted, orthopyroxene (Opx)-poor harzburgites to rare dunites. Micro-textures indicate a process partial dissolution of deformed Opx at the expenses of unstrained Ol and Cpx (Fig. 3). Importantly, Cpx occurs as small grains interstitial to Ol and often associated to Spl, or as megacrysts organized in cm-scale veinlets (Fig. 3). These textures show that Cpx crystallized during the last phases of the interaction process, in association with intergranular Spl having low Cr# (Fig. 4a) (see also Piccardo et al., 2007). Despite the local crystallization of Cpx, the gradual dissolution of Pl and addition of Ol led to a general decrease in bulk-rock Al_2O_3, CaO (Fig. 4d), and incompatible elements (i.e., TiO_2, Na_2O and K_2O, not shown) at increasing MgO. The replacive harzburgites are distinct from the concordant MORB-dunites in olivine and clinopyroxene having depleted incompatible trace element compositions, as portrayed in Figures 4b and 4c. Importantly, the clinopyroxene and olivine from these replacive bodies are geochemically more depleted than those in the host Pl-peridotites.

4. Sample selection and analytical mythologies

Three plagioclase(Pl)-peridotites, seven dunites and eight harzburgites from four MORB-like dunite and two depleted harzburgite replacive bodies were selected for the whole-rock PGE and Re-Os isotopic determinations in this study. Major and trace and Nd-Hf isotopic compositions of clinopyroxene from six depleted harzburgites and two Pl-peridotites are discussed in Sanfilippo et al. (2019). New trace and Nd-Hf isotopic compositions clinopyroxene from one additional Pl-peridotite and two Cpx-rich segregation from two MORB-type dunite bodies are also reported. The trace and isotopic compositions of the clinopyroxene (Tables S1 and S2) and the whole rock major, PGE and Re-Os isotope compsitions (Tables S3) are included as supplementary files.

Major element compositions of minerals were obtained using a JEOL JXA-8200 electron microprobe located at Dipartimento di Scienze della Terra, Università degli Studi di Milano (Italy). Conditions of analyses were 15 kV accelerating voltage and 15 nA beam current. Counting time was 30 s on the peak and 10 s on the backgrounds. Natural minerals were used as standards and data reduction was carried out using the CITZAF package.

Trace element compositions of clinopyroxene were obtained using Laser Ablation Inductively Coupled Plasma Mass Spectrometry (LA-ICPMS) at C.N.R., Istituto di Geoscienze e Georisorse (Unità di Pavia) using a PerkinElmerSCIEX ELAN DRC-e quadrupole mass spectrometer coupled with an UP213 deep-UV YAG Laser Ablation System (New Wave Research, Inc.). The laser was operated at a repetition rate of 10 Hz, with 213 nm wavelength and a fluence of ~9.5 J/cm^2. Spot diameter was 100 microns. NIST SRM 610 synthetic glass standards was used as external standard, CaO was used as internal standard. Precision and accuracy of the REE concentration values were assessed through repeated analysis of the BCR2-g standard to be better than ±7% and ±10%, respectively, at the ppm concentration level.

Isotopic composition of Nd and Hf of clinopyroxene, dissolution and column chemistry were done at the National High Magnetic Field Laboratory, Florida State University, using the same methodology reported in Sanfilippo et al. (2019). The clinopyroxene separates (~200 mg, hand-picked under binocular microscope) were leached in ~5 mL 2.5N HCl and ~500 μL <30% H_2O_2 for 20–30 min at room temperature to remove any alteration products. The leached separates were rinsed several times with quartz sub-boiling distilled water. Subsequent dissolution and column chemistry was performed after procedures described in Stracke et al. (2003). Nd, and Hf isotopes were measured using the Thermofisher NEPTUNE MultiCollector Inductively Coupled Plasma Mass Spectrometer (MC-ICPMS). The 143 Nd/144 Nd ratios are corrected for mass bias using ^{146}Nd/^{144}Nd ratio of 0.7219 and reported relative to La Jolla standard of 0.511850. Blanks for Nd were ~10 pg. The ^{176}Hf/^{177}Hf ratios are corrected for mass bias using ^{179}Hf/^{177}Hf ratio of

0.7325 and reported relative to JMC-475 value of $^{176}Hf/^{177}Hf$ = 0.282150. Blanks for Hf were <40 pg. Reproducibility of the LaJolla and JMC475 standards is similar to their in-run precision.

Whole rock Re-Os isotopes were analysed at the IGGCAS using the isotope dilution method (Chu et al., 2009). The detailed analytical procedure has been described in Liu et al. (2022). About 2 g powders, together with a ^{187}Re-^{190}Os spike and a mixed ^{191}Ir-^{99}Ru-^{194}Pt-^{105}Pd spike, were mixed in Carius tubes, which were digested with reverse aqua regia (i.e., 3 ml 12N HCl and 6 ml 16N HNO3) at 240 °C for ~72 hours in an oven. Osmium was extracted from the aqua regia solution by solvent extraction into CCl4 and further purified by micro-distillation (Birck et al., 1997). Other HSE were firstly separated from the solution into subgroups (Re–Ru, Ir–Pt, and Pd) using a 2 mL anion exchange resin (AG-1×8, 100–200 mesh). Subsequently, the Re–Ru was further purified by a 0.25 mL anion exchange resin; the Pd and Ir–Pt were further purified by an Eichrom LN spec resin to completely remove Zr and Hf.

Osmium concentrations and isotopes were measured by negative thermal ionization mass spectrometry (N-TIMS) on a Neptune Triton in a static mode using Faraday cups. A Ba(OH)2 solution was used as an ion emitter. The measured Os isotopes were corrected for mass fractionation using the $^{192}Os/^{188}Os$ ratio of 3.0827. The Nier oxygen isotope composition ($^{17}O/^{16}O$=0.0003708 and $^{18}O/^{16}O$=0.002045) has been used for oxide correction. The in-run precisions for Os isotopic measurements were better than 0.2% (2σ) for all the samples. Johnson-Matthey standard of UMD was used as an external standard, yielding a $^{187}Os/^{188}Os$ ratio of 0.11378±2 (2s; n=5). Concentrations of other HSE were measured on a Thermo Fisher Scientific Neptune MC-ICPMS with an electron multiplier in peak-jumping mode or using Faraday cups in static mode, depending on the measured signal intensity. In-run precisions for $^{185}Re/^{187}Re$, $^{191}Ir/^{193}Ir$, $^{99}Ru/^{101}Ru$, $^{194}Pt/^{196}Pt$, and $^{105}Pd/^{106}Pd$ were 0.1–0.3% (2 s). The Re, Ir, Ru, Pt, and Pd standards were used to correct mass fractionations. The total procedural blanks were 3 ± 1 pg for Os, 5 ± 2 pg for Re, 1 ± 0.5 pg for Ir, 10 ± 4 pg for Ru, 18 ± 9 pg for Pt, and 9 ± 4 pg for Pd (n=10). A $^{187}Os/^{188}Os$ ratio of ~ 0.15 was obtained for the blank. The standard UB-N was used to monitor the accuracy of the analytical procedure.

5. Results

Major, trace elements and Nd-Hf isotope compositions of Pl-peridotites and replacive harzburgite bodies were discussed by Sanfilippo et al. (2019). The Cpx trace element and Nd-Hf isotope compositions are here briefly summarized along with data from the new MORB-type dunites. The Cpx from the Pl-peridotites have chondrite-normalized REE patterns highly depleted in LREE (La_N/Sm_N=0.01-0.04) and with high M-HREE (15 times CI), and the incompatible element patterns characteristically displaying negative Sr anomaly (Sr/Sr*[(Ce_N*Pr_N)] =0.03-0.05) and low Zr_N/Hf_N ratios (0.3-0.4). The interstitial Cpx in the replacive MORB-type dunites are similar to Cpx in equilibrium with MORB, and distinct from those of the host Pl-peridotites in the higher LREE and lower H-MHREE contents. Some of the dunites include Cpx displaying highly variable L/MREE fractionations (La_N/Sm_N=0.20-1.13). In addition, the dunite Cpx does not have Sr negative anomaly (Sr/Sr*=0.9), in agreement with the lack of Pl, and have chondritic Zr/Hf ratios (Zr_N/Hf_N= 0.9). The Cpx in the depleted replacive harzburgites has distinctively depleted REE patterns characterized by low H-MREE contents (3-5 times CI), but typically higher L/MREE ratios (La_N/Sm_N=0.14-0.62). The Cpx in depleted replacive harzburgites lacks significant Sr negative anomaly (Sr/Sr*=0.7-1.6), similar to the MORB-type dunites, and exhibits a weak fractionation between Zr and Hf (Zr_N/Hf_N= 0.7-1.1).

The initial Nd-Hf isotopic compositions of Cpx are calculated at 160 Ma, following the age of the MORB-type magmatism in Lanzo, as evidenced by i) zircon U-Pb ages of the gabbros crosscutting the Lanzo South peridotites (Kaczmarec et al, 2008) and ii) Pl-Cpx-WR internal isochrons defined by two pyroxenites from Lanzo North (Sanfilippo et al., 2022). Early Jurassic ages (160 Ma) are also retrieved from two errorchrons provided by the Cpx in the replacive harzburgites, thought to be evidence of resetting of the Nd-Sm system during their formation

(Sanfilippo et al., 2019). The initial Nd and Hf isotopes of the Cpx in the host Pl-peridotites plot in the MORB field (Fig. 5). This agrees with the idea that these rocks experienced a nearly complete equilibration with MORB-like melts during the impregnation event (see Bodinier et al., 1991; Piccardo et al., 2007). The Cpx-rich segregations within the two MORB-type dunite also plots in the Nd-Hf isotopic field of present-day MORB, although their variability exceed that of basalts from the Alpine-Apennine ophiolites, which have a restricted Nd-Hf isotopic range (see Rampone and Sanfilippo, 2021 for a review). Sample LZ66 Cpx has less radiogenic Nd and Hf isotope compositions (ε_{Nd}= +4.2; ε_{Hf}= +8.0) compared to the host Pl-peridotites, whereas sample LZ31 Cpx has ε_{Nd} and ε_{Hf} similar to those of the host rocks (+7.8 and +11.8, respectively). On the other hand, Cpx in the depleted replacive harzburgites does not plot in the Nd-Hf isotope MORB field, having Hf isotopes extending by far any melts ever erupted at present-day Mid Ocean Ridges. These Cpx have highly radiogenic, yet variable Hf isotope compositions (εHf=40-220), coupled with MORB-like Nd isotopes. Similar isotopic compositions characterize other melt-reacted harzburgites from Lanzo North (Guarnieri et al., 2012) and were documented in abyssal peridotites from the Gakkel (Stracke et al., 2011) and the Mid Atlantic Ridge (Sani et al., 2023). In addition, highly radiogenic Hf isotopes have been documented in plume-related peridotites such as the Salt Lake Crater xenoliths from Hawaii (Bizimis et al., 2003, Salters and Zindler, 1985).

The three rock-types are also characterized by distinct whole-rock PGE-normalized patterns. The Pl-peridotites have nearly flat patterns approaching those of the PM, and thereby plotting in the fertile-end of the field of abyssal peridotites. Notably, they have higher Pd and Re compared to the subcontinental peridotites from Lanzo Nord (Becker et al., 2006) (Fig.6a), in agreement with their 're-enriched' geochemical nature. The MORB-type dunites are characterized by selective enrichments in Pd and, in some samples, Re relative to the host rocks, whereas the Ir and Pt are only slightly enriched compared to the Pl-peridotites (Fig.6b). Similar to Re, some samples also have Os higher than the host rocks (Fig. 4d). Take as a whole, the PGE patterns in the MORB-type dunites stand in the enriched field of the melt-infiltrated (i.e., S-enriched; Luguet et al., 2003) replacive rocks from present-day MOR. Unlike the replacive dunites, the depleted replacive harzburgites are distinct from the host Pl-peridotite in lower Pd and Re, whereas Os-Ir-Ru and Pt are nearly undistinguishable (Fig.6c). One sample was selected along the contact between the Pl-peridotites and the depleted harzburgites, and reveals PGE patterns undistinguishable from those of the Pl-peridotite (LZ205, Fig.c). Notably, Os, Re (Fig. 4d) and Re/Os ratios (Fig.7b) in the depleted harzburgites and Pl-peridotites correlates with the whole-rock Al_2O_3 contents (Fig.7a), whereas the MORB-type dunites display extremely variable Os, Re and Re/Os ratios (Figs. 4c, 7b), ranging from higher to lower values compared to the host Pl-peridotites (Fig.7a). Initial $^{187}Os/^{188}Os$ isotopes (calculated at 165 Ma) can also distinguish the two generations of replacive bodies. MORB-type dunites have initial $^{187}Os/^{188}Os$ ranging from 0.1221 to 0.1277 (Fig.7b), in the same range of the host Pl-peridotites (from 0.1221 to 0.126). The replacive harzburgites have highly variable initial $^{187}Os/^{188}Os$ (0.1178-0.1238), which decreases with decreasing Re/Os ratio, Al_2O_3 (Fig. 7a, b), CaO and incompatible element contents (not reported). The highest $^{187}Os/^{188}Os$ values of the replacive harzburgites are similar to those of the Pl-harzburgites. The Pl-peridotites and the depleted harzburgites have similar Ir/Pd ratios, invariably higher than PM, whereas the MORB-type dunites are distinct in Ir/Pd ratios lower than PM (Fig. 7c).

6. Discussion

6.1 Melt-peridotite reactions and preserved isotopic variability in MORB-type dunites

Our new Cpx trace elements and Nd-Hf compositions of the concordant dunites bodies coherently indicate migration of mantle melts with an N- to E-MORB geochemical affinity. In detail, Cpx in these rocks are selectively enriched in LREE compared to Cpx from the host Pl-peridotites (Fig. 4), and those in coeval lower crustal sections of the Alpine ophiolites (see also Piccardo et al., 2007). Likewise, the geochemical variability in Ol geochemistry in some of the MORB-type dunites point to a mildly enriched signature of the melts transported in these migration channels (Sanfilippo et al., 2014; 2017). Whole-rock PGE compositions of samples from 4 dunite bodies selected in this study show high PGE contents, having Pt and Pd contents higher than the host Pl-peridotites, but variable Os and Re contents (Fig. 6b). In particular, all the MORB-dunites are characterized by low Ir/Pd ratios (Fig. 7c), a geochemical signature interpreted to be derived by melt-mantle interaction (e.g., Baker et al., 2006; Marchesi et al., 2013; Reisberg, 2021). Low Ir/Pd ratios, for instance, characterize the plagioclase-rich dunites and Ol-rich troctolites from Central Indian Ridge (Sanfilippo et al. 2016), considered hybrid crustal lithologies formed at the expenses of former mantle peridotite intruded by migrating MORB melts (see also Tamura et al., 2016), and harzburgites from the mid-Atlantic Ridge modified by S-rich melts (Luguet et al, 2003).

At low pressure conditions, mantle melts are undersaturated in sulfides (Mavrogenes and O'Neill, 1999) and may preferentially dissolve interstitial radiogenic sulfides from a peridotite matrix. This process causes an increase in S and gradually enriches the $^{187}Os/^{188}Os$ ratios of the migrating melt (Sen et al., 2011). The subsequent crystallization of large quantities of olivine and spinel during the interaction process may drives the melt toward S saturation, which leads to the crystallization of magmatic sulfides having radiogenic O signature within the replacive body (Bézos et al., 2005). However, the extent to which the melt-reacted peridotite acquires the composition of the migrating melt depends on the efficiency of the crystallization process, i.e., the amount of newly formed sulfides crystallized during the interaction. Despite notable enrichments in Pd and, locally, in Os, the MORB-type dunites in this study have variable Re contents. This suggests that sulfides were added in different amounts within the different samples at the closure of the porosity, when the migrating melt is likely to have equilibrated with the original mantle matrix (see Reisberg 2021). In particular, we noted that the dunites with the lowest whole rock Al_2O_3 contents are depleted in Re relative to both Pt and Pd (Fig. 2), which are likely formed by extensive reaction with the migrating melts. Given the very low degrees of serpentinization in these samples (LOI<1%), the low Re cannot be attributed to secondary Re loss during hydrous alteration (Lorand et al., 2000). More likely, the relatively lithophile character of Re compared to other PGEs (Büchl et al., 2002; Becker et al., 2006; Fischer-Gödde et al., 2011) caused a limited Re retention in the newly crystallized solid sulphides (Reisberg et al., 2005). Indeed, the moderately incompatible character of Re causes its partitioning to be strongly controlled by melt/rock ratios (e.g., Dale et al., 2009; Fonseca et al., 2007), so that the accumulation of Re might have been prevented in samples formed by the total conversion of a Pl-peridotite to a dunite. On the other hand, the MORB-type dunites having high Re and Re/Os ratios also have high Al_2O_3 contents. These rocks likely formed at lower melt-rock ratio and, despite the addition of sulfides increased the overall I-PGE (i.e., Os, Ir and Ru) contents, their IPGE concentrations were mostly buffered by the former Pl-peridotites, acquiring $^{187}Os/^{188}Os$ similar to that of the host rocks.

This is further confirmed by the compositions of the two MORB-type dunites (i.e., LZ66 and LZ31) having Cpx-rich segregations, which reveal that the Nd-Hf isotopic variability agrees with the whole-rock Os isotope compositions. The Cpx in the two samples ranges from isotopic values identical to those of the host Pl-peridotites for sample LZ31 (ƐNd=7.8 and ƐHf=11.8) to less radiogenic than the host rocks for sample LZ66 (ε_{Nd} =4.2 and ε_{Hf} =7.5). Likewise, the Os isotope compositions of the two dunite bodies varies from relatively low ($^{187}Os/^{188}Os$=0.1221) to distinctively high values ($^{187}Os/^{188}Os$=0.1277) for LZ31 and LZ66, respectively. We thereby infer that the MORB-type replacive dunites acted as high-permeability migration pathways for mafic melts having slightly different isotopic compositions, nevertheless in line with the isotopic range of erupted MORB and of the host peridotites (Fig. 5).

6.2 Formation of depleted harzburgites as an incomplete melt-rock reaction process

Melt-peridotite interactions also had a leading effect on the composition of the depleted replacive harzburgites. These rocks have been interpreted as product of interaction between the host Pl-peridotites and a melt with ultra-depleted trace element compositions and highly radiogenic Nd-Hf isotopes (Sanfilippo et al., 2019). In the field, these bodies show gradational contacts with the Pl-peridotites, with evidence that the melt-rock reaction process produced a partial annealing of

354 the tectonite structure of the Pl-peridotites converted into isotropic harzburgites. In addition, the
355 harzburgite shows large, kinked Opx partly adsorbed by cm-sized undeformed olivine, and
356 interstitial Cpx associated with chromite having lower Cr# than those in the host rock (Fig. 4). The
357 field and textural evidences for a replacive origin are further supported by the chemistry of the
358 clinopyroxene. Compared to the Cpx in host Pl-peridotites, the interstitial Cpx in the harzburgites
359 has markedly lower M-HREE contents but higher and variable LREE, which result in overall flat
360 REE patterns characterized by low LREE/M-HREE fractionations (Fig. 4c). The lower M-HREE
361 contents of the Cpx in the depleted harzburgites compared to those of the host rocks require that
362 the migrating melts had a depleted geochemical signature, whereas the local enrichments in LREE
363 indicate that this mineral crystallized at a reduced porosity (see Piccardo et al., 2007; Sani et al.,
364 2020). Similarly, Cpx in all selected harzburgites retain highly radiogenic Hf isotope signatures,
365 coupled to less radiogenic $^{143}Nd/^{144}Nd$ ratios (Fig.5). Based on the replacive nature of these rocks,
366 Sanfilippo et al. (2019) proposed that the depleted incompatible trace elements and the Nd-Hf
367 isotopic signature were caused by incomplete interactions between melts having an ultra-depleted
368 affinity and the host Pl-peridotites. Hence, contrary to what proposed for the ultra-depleted mantle
369 peridotites sampled in oceanic environments (Liu et al., 2008; Bizimis et al., 2003; Stracke et al.,
370 2011; Byerly and Lassitier 2014; Tilhac et al., 2023; Sani et al., 2023), the ultra-depleted chemical
371 and isotopic signatures of the Cpx in the Lanzo replacive harzburgites might have been caused by
372 interactions with melts generated by ancient, refractory sources (Sanfilippo et al.,2019). The new
373 PGE and $^{188}Os/^{187}Os$ data in this study further sustain this idea.

374 The replacive harzburgites preserve covariations between whole-rock Re, Os, $^{188}Os/^{187}Os$,
375 and lithophile elements (see Fig. 4; Tables S3 and S4), which can be potentially attributed to a
376 process of ancient mantle melting followed by radiogenic Os ingrowth (Reisberg and Lorand,
377 1995; Harvey et al., 2006; Liu et al., 2008; Stracke et al., 2011; Luguet and Reisberg, 2016). In this
378 scenario, the PGE contents of the Lanzo peridotite would represent the starting peridotite,
379 preserving PM-like PGE compositions and gradually shift towards more refractory compositions

during old event of melt-extraction (see also Becker et al., 2006). If this was the case, however, the high MgO contents of the replacive harzburgite would indicate a strongly refractory character, well above the sulfur saturation point. However, the refractory harzburgites reveal depletions in only in Re, whereas Pd, Pt, Ru and Ir are similar to those of the host Pl-peridotites, much higher than the PGE patterns expected for residues at high melting degrees (see Fig. 6). Indeed, unlike residues of mantle melting, the fractionation between Ir and Pd (Fig. 7), or Pt (not shown) is nearly constant in all Lanzo harzburgites, and similar to those of the host Pl-harzburgites, despite the large variations in Al_2O_3 contents would require large variations in melting degrees. Hence, with the exception of Os and Re, the overall PGE variations in the refractory harzburgites is at odds with melting trends. In this light, the increase in depletion indexes at increasing Os and decreasing Re can be related to a reactive melt-rock migration process (Reisberg, 2021). For instance, the percolation of a mafic melts along the grain boundaries might have promoted a gradual removal of interstitial sulfides, rich in Re and having high $^{187}Os/^{188}Os$ (Alard et al., 2002; Luguet et al., 2003; Harvey et al., 2006; Marchesi et al., 2014). A subsequent melt with an ultra-depleted geochemical nature could have been associated with the local addition of Os-rich, unradiogenic sulfides (Day et al., 2017) derived from melting ancient portions of the mantle asthenosphere, similar to the abyssal peridotites characterized by highly radiogenic Hf isotopes (Byerly and Lassitier, 2014; Stracke et al., 2019; Sani et al., 2023). Indeed, even if unradiogenic Os sulfides are generally found as inclusions within the silicate phase, experimental studies indicate that the grain boundary diffusivity of Os can be several orders of magnitude higher than other lithophile elements (e.g., Hayyden and Watson, 2007). Hence, at asthenospheric temperatures and given enough time the original Os isotopic signature can be partly or totally redistributed amongst the different sulfide populations in a sample that suffered old events of melting or melt-rock reaction (Reisberg, 2021). For instance, this is shown by the preservation of low Os, skeletal sulfides with relatively high Re/Os but unradiogenic $^{187}Os/^{188}Os$ in refractory abyssal peridotites (0.117; Harvey et al., 2006). Hence, the unradiogenic

Os signature of ancient melting residues can be potentially transferred to their primary melts, along with highly radiogenic Hf and Nd isotope compositions.

Another argument in favour of a replacive, rather than residual, origin of the harzburgites is the relationship between whole rock $^{188}Os/^{187}Os$ and the Cpx ε_{Hf} (Fig. 8). The sample from the depleted replacive harzburgite retaining the lowest $^{188}Os/^{187}Os$, and less depleted whole rock compositions, also has the highest Cpx ε_{Hf}. On the other hand, those retaining the most depleted compositions in term of whole rock and Cpx ε_{Hf} have the highest $^{188}Os/^{187}Os$. Mantle melting causes increases in Lu/Hf ratios, coupled to synchronous removal of Re, which, will develop a highly radiogenic Hf isotopes associated with low $^{188}Os/^{187}Os$with time. Such a relationship is manifested by the Gakkel peridotites, considered ancient residues of partial melting (Fig. 8) (Liu et al., 2008; Stracke et al., 2011). On the other hand, a conversion of a Pl-peridotites into refractory harzburgites causes the assimilation of plagioclase and interstitial sulfides, thus lowering the whole rock in Al, Ca and incompatible elements contents, along with Re. During the first stages of this melt-mantle interaction process, the melt-reacted peridotite retains a less refractory whole-rock composition, but the migrating melt preserves its original radiogenic signature due to limited chemical equilibration with the host rock. Hence, the crystallizing Cpx retains the composition of the migrating melt, poor in incompatible elements and preserving a radiogenic Hf isotopic signature. Indeed, the intergranular texture and the high LREE/M-HREE ratios of the Cpx the in harzburgites indicate that this mineral crystallized directly from the migrating melt, at the closure of the permeability (see Dygert and Liang, 2015). While whole-rock PGE contents and Os isotope ratios are buffered towards those of the unreacted peridotite, the Cpx would thereby preserve the geochemical fingerprint of the migrating melt. As the melt-rock reaction proceed, the peridotite becomes gradually more refractory (low Al and Ca contents, low Re and low $^{187}Os/^{188}Os$; see also Reisberg et al., 2021), but the melt has interacted extensively with the host rock, shifting the Hf-Nd isotopic compositions of the crystallizing Cpx towards that of the host peridotite. Different degrees of melt-rock reactions, thereby, may produce the correlations between Os and Hf isotopes observed for the Lanzo replacive harzburgites. We note that the correlation in Figure 8 can be preserved only if the reacting melt is geochemically more depleted than the host peridotites, a combination fortuitously preserved in the Jurassic Lanzo ophiolite (see McCarthy and Muntener, 2019; Rampone and Sanfilippo, 2021), but definitely unusual at a mature Mid Ocean Ridge.

6.3 Melt migration in chemically isolated melt pathways

Our results suggest that magma mixing inside the replacive dunite channels in Lanzo was limited. In particular, rather than enriched magmas from fertile mantle component, we document that channelized magma transport mainly preserved melts from refractory lithologies, witnesses of ancient melting events. The efficiency of melt mixing is dependent both on the length scale of the heterogeneity and on the velocity of magma transport (Liu and Liang, 2017). In particular, if mantle heterogeneities are small, the chemical signature of primary magmas can be easily diluted soon after their creation. On the other hand, heterogeneity can be better preserved if the size of the heterogeneity is large enough to limit efficient mixing during transport. It is therefore likely that these refractory mantle components were large enough to generate their own network of channels to account for preservation of isotopic heterogeneity. On the other hand, our study reveals that primary melts from more fertile lithologies were more efficiently mixed during melt transport (Stracke and Bourdon, 2009), forming a network in the dunite with isotopic and trace element compositions plotting in the field of MORB. This can be related either to the size of these enriched endmember, or to the fat that melts from fertile materials are more prone to melt–rock reactions with the ambient depleted peridotites (Lambart et al., 2009) and their occurrence can easily nucleate channelization (Weatherley and Katz, 2012; Liu and Liang, 2019). In both cases, the MORB-type replacive dunites preferentially transport melts from the most fusible component in the lowermost part of the melting region, efficiently mixed with melts from DM-like lithologies. On the other hand, ultra-depleted melts from ancient mantle were transported in chemically isolated pathways. Despite their refractory character, thermodynamic models showed that depleted mantle peridotites retaining ancient traces of melt depletion can produce substantial amount of melts before exhaustion of Cpx (Byerly and Lassiter, 2014; Sani et al., 2020), in agreement with the local occurrence of ultra-depleted isotopic compositions in olivine melt inclusions form the Azores (Stracke et al., 2019), and with the local occurrence of erupted MORB having anomalously high Hf isotopes (Blichert-Toft et al., 2005; Salters et al., 2011; Sanfilippo et al., 2021). However, melting of such lithologies requires substantially lower pressures, thereby discouraging mixing between magmas derived from more enriched components and preserving their extreme isotopic compositions. Hence, the ultra-depleted geochemical signature of melts from ancient refractory mantle lithologies has a higher chance to be preserved within shallow migration channels, such as the discordant replacive mantle bodies of Lanzo.

Despite magma chambers processes have a leading effect in mixing and averaging the primitive magma compositions, further concurrence with our hypothesis comes from recent investigations on abyssal gabbros. For instance, the widespread occurrence high anorthite plagioclase in gabbros and in crystal cargoes of MORB indicate that the contribution of ultra-depleted mantle lithologies is by far higher than that revealed by erupted MORB (Neave and Namur, 2020). Furthermore, significant variations in Nd and Sr isotopes are preserved in crystal cores from some primitive gabbros from the Atlantis Massif core complex, at Mid Atlantic Ridge (Lambart et al, 2019). These variations encompass the range of isotopic variability of erupted MORB in the entire MAR, and provide evidence that melts from a heterogeneous mantle were delivered to the lower crust before extensive mixing. On this basis, we conclude that the preserved Nd-Hf-Os isotopic variability that we document in the Lanzo replacive bodies can be a common feature in melt migration channels within the abyssal mantle. This implies that the limited isotopic variability recorded by erupted MORB is mainly the consequence of mixing crustal-level. In particular, melts from ancient and depleted mantle portions have high chance to be delivered towards the crust-mantle boundary with limited extent of aggregation. Critical is thereby the definition of the degrees of chemical heterogeneity of lower crustal reservoirs, before magma mixing and melt-rock reaction further complicate the transfer of the original mantle heterogeneity to the erupted melts.

7. Concluding remarks

This study documents a complete geochemical characterization of two generations of decametre-scale replacive mantle bodies from the Jurassic Lanzo South ophiolite, Western Italian Alps. We show that these replacive bodies can be considered migration pathways for primitive mantle melts produced during the opening of the Ligurian-Piedmontese basin. The Cpx and Ol in the MORB-dunites point to a mildly enriched signature of the melts transported in these migration channels, and is also indicated by the high PGE contents and radiogenic $^{187}Os/^{188}Os$ ratios (0.122-0.128). The discordant harzburgites, on the other hand, are geochemically depleted, and have Hf isotopes Cpx extending by far the isotopic variability of erupted MORB. Preserved correlations between PGE, Os isotopes and whole-rock compositions are dependent on melt-rock reaction and indicate that the depleted character was inherited from the migrating melt. In essence, the MORB-like dunite experienced the migrations of melts having variable contributions from enriched lithologies, already partly mixed with melts from DM-peridotites. The depleted harzburgites, instead, mostly acted as migration pathways for melts sourced by ancient, highly depleted lithologies. Therefore, we postulate that melts from ancient and depleted mantle portions have higher chance to be delivered towards the crust-mantle boundary with limited extent of aggregation. If the preserved Nd-Hf-Os isotopic variability documented in the Lanzo replacive bodies is a common feature in melt migration mantle channels, this implies that magma mixing at deep crustal levels may have a primary, hitherto poorly recognized role in determining the chemical heterogeneity of erupted melts. Hence, the chemical heterogeneity of lower crustal reservoirs needs to be better characterized in order to understand to what extent the original mantle heterogeneity is transferred to the erupted basalts.

Acknowledgments

We thank S. Tamburelli and Nicolò Rizzo for their assistance in fieldwork, mineral separation and isotope analyses. This work was financially supported by two Programma di Rilevante Interesse Nazionale (PRIN Prot. 2015C5LN35) to R. Tribuzio and (PRIN Prot.2017KX5ZX8) to A. Sanfilippo. Part of this work was performed at the National High Magnetic Field Laboratory, which is supported by National Science Foundation Cooperative Agreement No. DMR-1157490 and the State of Florida.

References

Aharonov, E., Whitehead, J. A., Kelemen, P. B., & Spiegelman, M. (1995). Channeling instability of upwelling melt in the mantle. Journal of Geophysical Research: Solid Earth, 100(B10), 20433-20450.

Alard, O., Griffin, W.L., Pearson, N., Lorand, J.P., O'Reilly, S.Y. (2002). New insights into the Re-Os systematics of sub-continental lithospheric mantle from in-situ analyses of sulfides. Earth Planet. Sci. Lett. 203, 651–663.

Alard, O., Luguet, A., Pearson, N.J., Griffin, W.L., Lorand, J.-P., Gannoun, A., Burton, K.W., O'Reilly, S. (2005. In situ Os isotopes in abyssal peridotites bridge the isotopic gap between MORBs and their source mantle. Nature 436, 1005–1008.

Akizawa N., Ozawa K., Tamura A., Michibayashi K. and Arai S. (2016). Three dimensional evolution of melting, heat and melt transfer in ascending mantle beneath a fast-spreading ridge segment constrained by trace elements in clinopyroxene from concordant dunites and host harzburgites of the Oman ophiolite. J. Petrol. 57, 777–814.

Becker H., Horan M. F., Walker R. J., Gao S., Lorand J.-P. and Rudnick R. L. (2006) Highly siderophile element composition of the Earth's primitive upper mantle: Constraints from new data on peridotite massifs and xenoliths. Geochim. Cosmochim. Acta 70, 4528–4550.

Bézos, A., Lorand, J. P., Humler, E., & Gros, M. (2005). Platinum-group element systematics in Mid-Oceanic Ridge basaltic glasses from the Pacific, Atlantic, and Indian Oceans. Geochimica et Cosmochimica Acta, 69(10), 2613-2627.

Birck, J.L., Roy-Barman, M., Capmas, F. (1997). Re-Os isotopic measurements at the femtomole level in natural samples. Geostandard Newsletters 21, 19-27.

Bizimis, M., Sen, G., & Salters, V. J. M. (2003). Hf–Nd isotope decoupling in the oceanic lithosphere. Constraints from spinel peridotites from Oahu, Hawaii. Earth and Planetary Science Letters, 217(1–2), 43–58. https://doi.org/10.1016/S0012-821X(03)00598-3

Blichert-Toft, J., Chauvel, C., & Albarède, F. (1997). Separation of Hf and Lu for high-precision isotope analysis of rock samples by magnetic sector-multiple collector ICP-MS. Contributions to Mineralogy and Petrology, 127(3), 248–260. https://doi.org/10.1007/s004100050278

Bodinier, J.L., Menzies, M.A., Thirlwall, M.F., 1991. Continental to Oceanic Mantle Transition: REE and Sr–Nd Isotopic Geochemistry of the Lanzo Lherzolite Massif. J. Petrol., Special Lherzolite Issue, pp. 191–210.

Boudier F. (1978) Structure and petrology of the Lanzo peridotite massif (Piedmont Alps). Geol. Soc. Am. Bull. 89, 1574–1591.

Boudier F. and Nicolas A. (1977) Structural controls on partial melting in the Lanzo peridotites. Oreg. Dep. Geol. Miner. Ind. 96, 63–78.

Buchl A., Brugmann G. E. and Batanova V. G. (2004) Formation of podiform chromitite deposits: implications from PGE abundances and Os isotopic compositions of chromites from the Troodos complex. Cyprus. Chem. Geol. 208, 217–232.

Byerly, B. L., & Lassiter, J. C. (2014). Isotopically ultradepleted domains in the convecting upper mantle: Implications for MORB petrogenesis. Geology, 42(3), 203–206. https://doi.org/10.1130/G34757.1

Chu, Z.Y., Wu, F.Y., Walker, R.J., Rudnick, R.L., Pitcher, L., Puchtel, I.S., Yang, Y.H., Wilde, S. 2009. Temporal Evolution of the Lithospheric Mantle beneath the Eastern North China Craton. Journal of Petrology 50, 1857-1898.

Cipriani, A., Brueckner, H. K., Bonatti, E., & Brunelli, D. (2004). Oceanic crust generated by elusive parents: Sr and Nd isotopes in basaltperidotite pairs from the Mid-Atlantic Ridge. Geology, 32(8), 657–660. https://doi.org/10.1130/G20560.1

Day, J. M., Walker, R. J., & Warren, J. M. (2017). 186Os–187Os and highly siderophile element abundance systematics of the mantle revealed by abyssal peridotites and Os-rich alloys. Geochimica et Cosmochimica Acta, 200, 232–254. https://doi.org/10.1016/j.gca.2016.12.013

Dygert, N., & Liang, Y. (2015). Temperatures and cooling rates recorded in REE in coexisting pyroxenes in ophiolitic and abyssal peridotites. Earth and Planetary Science Letters, 420, 151-161.Fischer-Go¨dde M., Becker H. and Wombacher F. (2011) Rhodium, gold and other highly siderophile elements in orogenic peridotites and peridotite xenoliths. Chem. Geol. 280, 365–383.

Grove, T. L., Kinzler, R. J., & Bryan, W. B. (1992). Fractionation of mid-ocean ridge basalt (MORB). Washington DC American Geophysical Union Geophysical Monograph Series, 71, 281-310.

Guarnieri, L., Nakamura, E., Piccardo, G. B., Sakaguchi, C., Shimizu, N., Vannucci, R., & Zanetti, A. (2012). Petrology, trace element and Sr, Nd, Hf isotope geochemistry of the North Lanzo peridotite massif (Western Alps, Italy). Journal of Petrology, 53(11), 2259–2306. https://doi.org/ 10.1093/petrology/egs049

Harvey, J., Gannoun, A., Burton, K. W., Rogers, N. W., Alard, O., & Parkinson, I. J. (2006). Ancient melt extraction from the oceanic upper mantle revealed by Re–Os isotopes in abyssal peridotites from the mid-Atlantic ridge. Earth and Planetary Science Letters, 244(3–4), 606–621. https://doi.org/10.1016/j.epsl.2006.02.031

Harvey, J., Dale, C.W., Gannoun, A., Burton, K.W., 2011. Osmium mass balance in peridotite and the effects of mantle-derived sulphides on basalt petrogenesis. Geochim. Cosmochim. Acta 75, 5574–5596. https://doi.org/10.1016/j. gca.2011.07.001.

Hayden, L.A., Watson, E.B., 2007. A diffusion mechanism for core–mantle interaction. Nature 450, 709–711. https://doi.org/10.1038/nature06380.

Kaczmarek M. A. and Müntener O. (2010) The variability of peridotite composition across a mantle shear zone (Lanzo massif, Italy): interplay of melt focusing and deformation. Contrib. Mineral. Petrol. 160, 663–679.

Kaczmarek M. A., Müntener O. and Rubatto D. (2008) Trace element chemistry and U-Pb dating of zircons from oceanic gabbros and their relationship with whole rock composition (Lanzo, Italian Alps). Contrib. Mineral. Petrol. 155, 295–312.

Katz, R. F., & Weatherley, S. M. (2012). Consequences of mantle heterogeneity for melt extraction at mid-ocean ridges. Earth and Planetary Science Letters, 335, 226-237.

Kelemen P. B., Shimizu N. and Salters V. J. M. (1995) Extraction of mid-ocean-ridge basalt from the upwelling mantle by focused flow of melt in dunite channels. Nature 375, 747–753. http://dx. doi.org/10.1038/375747a0.

Kelemen P. B., Hirth G., Shimizu N., Spiegelman M. and Dick H. J. B. (1997) A review of melt migration processes in the adiabatically upwelling mantle beneath oceanic spreading ridges. Philos. Trans. R. Soc. Lond. A 355, 283–318..

Gagnon J. E., Fryer B. J., Samsona I. M. and Williams-Jones A. E. (2008) Quantitative analysis of silicate certified reference materials by LA-ICPMS with and without an internal standard.

Langmuir, C. H., Klein, E. M., & Plank, T. (1992). Petrological systematics of mid-ocean ridge basalts: Constraints on melt generation beneath ocean ridges. Mantle Flow and Melt Generation at Mid-Ocean Ridges, 183–280. https://doi.org/10.1029/gm071p0183

Lassiter, J. C., Byerly, B. L., Snow, J. E., & Hellebrand, E. (2014). Constraints from Os-isotope variations on the origin of Lena Trough abyssal peridotites and implications for the composition and evolution of the depleted upper mantle. Earth and Planetary Science Letters, 403, 178–187. https://doi.org/10.1016/j.epsl.2014.05.033

Liang, Y., Schiemenz, A., Hesse, M. A., & Parmentier, E. M. (2011). Waves, channels, and the preservation of chemical heterogeneities during melt migration in the mantle. Geophysical Research Letters, 38(20)

Liang Y. and Parmentier E. M. (2010) A two-porosity double lithology model for partial melting, melt migration and meltrock reaction in the mantle: the nature of channel melt and the role of matrix dissolution. J. Petrol. 51, 125–152. http://dx.doi. org/10.1093/petrology/egp086.

Liu, B., & Liang, Y. (2017). The prevalence of kilometer-scale heterogeneity in the source region of MORB upper mantle. Science Advances, 3(11). https://doi.org/10.1126/sciadv.1701872

Liu, B., & Liang, Y. (2019). Importance of permeability and deep channel network on the distribution of melt, fractionation of REE in abyssal peridotites, and U-series disequilibria in basalts beneath mid-ocean ridges: A numerical study using a 2D double-porosity model. Earth and Planetary Science Letters, 528, 115788. https://doi.org/10.1016/j.epsl.2019.115788

Liu C.-Z., J.E. Snow, G. Brugmann, E. Hellebrand, A.W. Hofmann (2009). Non-chondritic HSE budget in Earth's upper mantle evidenced by abyssal peridotites from Gakkel Ridge (Indian Ocean) Earth Planet. Sci. Lett., 283, pp. 122-132

Liu, C. Z., Dick, H. J., Mitchell, R. N., Wei, W., Zhang, Z. Y., Hofmann, A. W., et al. (2022). Archean cratonic mantle recycled at a mid-ocean ridge. Science Advances, 8(22), eabn6749. https://doi.org/10.1126/sciadv.abn6749

Lorand, J. P., Schmidt, G., Palme, H., & Kratz, K. L. (2000). Highly siderophile element geochemistry of the Earth's mantle: new data for the Lanzo (Italy) and Ronda (Spain) orogenic peridotite bodies. Lithos, 53(2), 149-164

Luguet A., J.-P. Lorand, M. Seyler (2003). Sulfide petrology and highly siderophile element geochemistry of abyssal peridotites: a coupled study of samples from the Kane Fracture Zone (45 W 23 20N, MARK Area, Atlantic Ocean) Geochim. Cosmochim. Acta, 67, pp. 1553-1570

Luguet A., Alard O., Lorand J. P., Pearson N. J., Ryan C. and O'Reilly S. Y. (2001) Laser-ablation microprobe (LAM)-ICPMS unravels the highly siderophile element geochemistry of the oceanic mantle. Earth Planet. Sci. Lett. 189, 285–294.

Luguet, A., Reisberg, L., 2016. Highly siderophile element and 187Os signatures in noncratonic basalt-hosted peridotite xenoliths: unravelling the origin and evolution of the post-archean lithospheric mantle. Rev. Mineral. Geochem. 81, 305–367. https:// doi.org/10.2138/rmg.2016.81.06.

Mallick, S., Dick, H. J., Sachi-Kocher, A., & Salters, V. J. (2014). Isotope and trace element insights into heterogeneity of subridge mantle.Geochemistry, Geophysics, Geosystems, 15(6), 2438–2453. https://doi.org/10.1002/2014gc005314

Mallick, S., Standish, J. J., & Bizimis, M. (2015). Constraints on the mantle mineralogy of an ultra-slow ridge: Hafnium isotopes in abyssal peridotites and basalts from the 9–25 E Southwest Indian Ridge. Earth and Planetary Science Letters, 410, 42–532. https://doi.org/10.1016/j.epsl. 2014.10.048

Marchesi C., Garrido C. J., Harvey J., Gonzalez-Jimenez J. M., Hidas K., Lorand J. P. and Gervilla F. (2013) Platinum-group elements, S, Se and Cu in highly depleted abyssal peridotites from the Mid-Atlantic Ocean Ridge (ODP Hole 1274A): influence of hydrothermal and magmatic processes. Contrib. Mineral. Petrol. 166, 1521–1538. http://dx.doi.org/10.1007/ s00410-013-0942-x.

Marchesi C., C.W. Dale, C.J. Garrido, D.G. Pearson, D. Bosch, J.L. Bodinier, F. Gervilla, K. Hidas Fractionation of highly siderophile elements in refertilized mantle: implications for the Os isotope composition of basalts. Earth Planet. Sci. Lett., 400 (2014), pp. 33-44

Martin C. E. (1991) Osmium isotopic characteristics of mantlederived rocks. Geochim. Cosmochim. Acta 55, 1421–1434.

McCarthy, A., & Müntener, O. (2019). Evidence for ancient fractional melting, cryptic refertilization and rapid exhumation of Tethyan mantle (Civrari Ophiolite, NW Italy). Contributions to Mineralogy and Petrology, 174(8), 69

Morgan Z. and Liang Y. (2005) An experimental study of the kinetics of lherzolite reactive dissolution with applications to melt channel formation. Contrib. Mineral. Petrol. 150, 369–385.

Morishita, T., Tani, K., Shukuno, H., Harigane, Y., Tamura, A., Kumagai, H., & Hellebrand, E. (2011). Diversity of melt conduits in the Izu-Bonin-Mariana forearc mantle: Implications for the earliest stage of arc magmatism. Geology, 39(4), 411-414.

Müntener O. and Manatschal G. (2006) High degrees of melting recorded by spinel harzburgites of the Newfoundland margin: The role of inheritance and consequences for the evolution of the southern North Atlantic. Earth Planet. Sci. Lett. 252, 437452.

Müntener O., Piccardo G. B., Polino R. and Zanetti A. (2005) Revisiting the Lanzo peridotite (NW-Italy): ‘‘asthenospherization” of ancient mantle lithosphere. Ofioliti 30, 111–124.

Müntener O., Manatschal G., Desmurs L. and Pettke T. (2010) Plagioclase peridotites in ocean–continent transitions: refertilized mantle domains generated by melt stagnation in the shallow mantle lithosphere. J. Petrol. 51(1–2), 255–294.

Neave, D. A., & Namur, O. (2022). Plagioclase archives of depleted melts in the oceanic crust. Geology, 50(7), 848-852

Xiong, Q., Xu, Y., Gonzalez-Jimenez, J.M., Liu, J.G., Alard, O., Zheng, J.P., Griffin, W.L., O'Reilly. 2022. Sulfide in dunite channels reflects long-distance reactive migration of mid-ocean-ridge melts from mantle source to crust: A Re-Os isotopic perspective. Earth and Planetary Science Letters 531, 115969.

Piccardo G. B., Zanetti A. and Mu¨ntener O. (2007) Melt/peridotite interaction in the Southern Lanzo peridotite: field, textural and geochemical evidence. Lithos 94, 181–209.

Quick, J. E. (1981). Petrology and petrogenesis of the Trinity peridotite, an upper mantle diapir in the eastern Klamath Mountains, northern California. Journal of Geophysical Research: Solid Earth, 86(B12), 11837-11863.

Rampone, E., & Sanfilippo, A. (2021). The heterogeneous Tethyan oceanic lithosphere of the Alpine ophiolites. Elements: An International Magazine of Mineralogy, Geochemistry, and Petrology, 17(1), 23-28

Rehkamper M., Halliday A. N., Alt J., Fitton J. G., Zipfel J. and Takazawa E. (1999) Non-chondritic platinum-group element ratios in oceanic mantle lithosphere: petrogenetic signature or melt percolation? Earth Planet. Sci. Lett. 172, 65–81.

Reisberg, L., Lorand, J.-P., 1995. Longevity of sub-continental mantle lithosphere from osmium isotope systematics in orogenic peridotite massifs. Nature 376, 159–162.

Reisberg, L., Zhi, X., Lorand, J.-P., Wagner, C., Peng, Z., Zimmermann, C., 2005. Re-Os and S systematics of spinel peridotite xenoliths from east Central China: evidence for contrasting effects of melt percolation. Earth Planet. Sci. Lett. 239, 286–308.

Reisberg, L. 2021. Osmium isotope constraints on formation and refertilization of the non-cratonic continental mantle lithosphere. Chmical Geology, 574, 120245, https://doi.org/10.1016/j.chemgeo.2021.120245

Rubatto D., Gebauer D. and Fanning M. (1998) Jurassic formation and Eocene subduction of the Zermatt-Saas-fee ophiolites: implications for the geodynamic evolution of the central and Western Alps. Contrib. Miner. Petrol. 132, 269–287.

Rudge, J. F., Maclennan, J., & Stracke, A. (2013). The geochemical consequences of mixing melts from a heterogeneous mantle. Geochimica et Cosmochimica Acta, 114, 112–143. https://doi.org/10.1016/j.gca.2013.03.042

Salters, V. J. M., & Zindler, A. (1995). Extreme176 Hf/ 177 Hf in the sub-oceanic mantle. Earth and Planetary Science Letters, 129(1–4), 13–30.https://doi.org/10.1016/0012-821X(94)00234-P

Salters, V.J.M., Dick, H.J.B., 2002. Mineralogy of the mid-ocean-ridge basalt source from neodymium isotopic composition of abyssal peridotites. Nature 418, 68–72.

Salters, V.J.M., Dick, H.J.B., 2011. Ultra depleted mantle at the Gakkel Ridge based on Hafnium and Neodymium isotopes. Eos Trans. AGU, Fall Meeting Suppl. 92. V41G-02.

Salters, V.J.M., Mallick, S., Hart, S.R., Langmuir, C.H., Stracke, A., 2011. Domains of depleted mantle; new evidence from hafnium and neodymium isotopes. Geochem. Geophys. Geosyst. https://doi.org/10.1029/2011GC003617.

Salters, V.J.M., Stracke, A., 2004. Composition of the depleted mantle. Geochem. Geophys. Geosyst. 5, Q05B07. https://doi.org/10.1029/2003GC000597.

Sanfilippo A., Tribuzio R. and Tiepolo M. (2014) Mantle–crust interaction in the oceanic lithosphere: constraints from minor and trace elements in olivine. Geochim. Cosmochim. Acta 141, 423–439.

Sanfilippo, A., Tribuzio, R., Ottolini, L., & Hamada, M. (2017). Water, lithium and trace element compositions of olivine from Lanzo South replacive mantle dunites (Western Alps): New constraints into melt migration processes at cold thermal regimes. Geochimica et Cosmochimica Acta, 214, 51-72.

Sanfilippo, A., Salters, V., Tribuzio, R., & Zanetti, A. (2019). Role of ancient, ultra-depleted mantle in Mid-Ocean-Ridge magmatism. Earth and Planetary Science Letters, 511, 89–98. https://doi.org/10.1016/j.epsl.2019.01.018

Sanfilippo, A., Salters, V. J. M., Sokolov, S. Y., Peyve, A. A., & Stracke, A. (2021). Ancient refractory asthenosphere revealed by mantle remelting at the Arctic Mid Atlantic Ridge. Earth and Planetary Science Letters, 566, 116981. https://doi.org/10.1016/j.epsl.2021.116981

Sani, C., Sanfilippo, A., Ferrando, C., Peyve, A. A., Skolotonev, S. G., Muccini, F., et al. (2020). Ultra-depleted melt refertilization of mantle peridotites in a large intra-transform domain (Doldrums Fracture Zone; 7–8°N, Mid Atlantic Ridge). Lithos, 374, 105698. https://doi.org/10.1016/j. lithos.2020.105698

Sani, C., Sanfilippo, A., Peyve, A. A., Genske, F., & Stracke, A. (2023). Earth mantle's isotopic record of progressive chemical depletion. AGU Advances, 4(2), e2022AV000792

Sen, I. S., Bizimis, M., Sen, G., & Huang, S. (2011). A radiogenic Os component in the oceanic lithosphere? Constraints from Hawaiian pyroxenite xenoliths. Geochimica et Cosmochimica Acta, 75(17), 4899-4916

Snow, J. E., & Reisberg, L. (1995). Os isotopic systematics of the MORB mantle: results from altered abyssal peridotites. Earth and Planetary Science Letters, 133(3-4), 411-421.

Snow, J. E., Hart, S. R., & Dick, H. J. (1994). Nd and Sr isotope evidence linking mid-ocean-ridge basalts and abyssal peridotites. Nature, 371(6492), 57–60. https://doi.org/10.1038/371057a0

Sobolev, A.V., Shimizu, N., 1993. Ultra-depleted primary melt included in an olivine from the Mid-Atlantic ridge. Nature 363, 151–154.

Spiegelman M. and Kelemen P. B. (2003) Extreme chemical variability as a consequence of channelized melt transport. Geochem. Geophys. Geosyst. 4, doi:1029/2002GC000336.

Spiegelman M., Kelemen P. B. and Aharonov E. (2001) Causes and consequences of flow organization during melt transport: the reaction infiltration instability in compactable media. J. Geophys. Res. 106, 2061–2077. http://dx.doi.org/10.1029/ 2000JB900240.

Standish J. J., Hart S. R., Blusztajn J., Dick H. J. B. and Lee K. L. (2002) Abyssal peridotite osmium isotopic compositions from Cr-spinel. Geochem. Geophy. Geosy. 3. http://dx.doi.org/10.1029/2001GC000161.

Stracke, A., 2012. Earth's heterogeneous mantle: a product of convection-driven interaction between crust and mantle. Chem. Geol. 330–331, 274–299.

Stracke, A., Bizimis, M., Salters, V.J.M., 2003. Recycling of oceanic crust: quantitative constraints. Geochem. Geophys. Geosyst. 4, 8003. https://doi.org/10.1029/ 2001GC000223.

Stracke, A., Bourdon, B., 2009. The importance of melt extraction for tracing mantle heterogeneity. Geochim. Cosmochim. Acta 73, 218–238.

Stracke, A., Snow, J.E., Hellebrand, E., von der Handt, A., Bourdon, B., Birbaum, K., Gunther, G., 2011. Abyssal peridotite Hf isotopes identify extreme mantle depletion. Earth Planet. Sci. Lett. 308, 359–368.

Stracke, A., Genske, F., Berndt, J., & Koornneef, J. M. (2019). Ubiquitous ultra-depleted domains in Earth's mantle. Nature Geoscience, 12(10), 851–855. https://doi.org/10.1038/s41561-019-0446-z

Suhr G. (1999) Melt migration under oceanic ridges: Inferences from reactive transport modelling of upper mantle hosted dunites. J. Petrol. 40, 575–599.

Tamura, A., Morishita, T., Ishimaru, S., Hara, K., Sanfilippo, A., & Arai, S. (2016). Compositional variations in spinel-hosted pargasite inclusions in the olivine-rich rock from the oceanic crust–mantle boundary zone. Contributions to Mineralogy and Petrology, 171, 1-14

Tilhac, R., Begg, G. C., O'Reilly, S. Y., & Griffin, W. L. (2022). A global review of HfNd isotopes: New perspectives on the chicken-and-egg problem of ancient mantle signatures. Chemical Geology, 121039

Wanless, V. D., & Shaw, A. M. (2012). Lower crustal crystallization and melt evolution at mid-ocean ridges. Nature Geoscience, 5(9), 651-655.

Warren, J. M. (2016). Global variations in abyssal peridotite compositions. Lithos, 248–251, 193–219. https://doi.org/10.1016/j.lithos.2015.12.023

Warren, J. M., Shimizu, N., Sakaguchi, C., Dick, H. J. B., & Nakamura, E. (2009). An assessment of upper mantle heterogeneity based on abyssal peridotite isotopic compositions. Journal of Geophysical Research, 114(B12), B12203. https://doi.org/10.1029/2008JB006186

Workman R. K. and Hart S. R. (2005) Major and trace element composition of the depleted MORB mantle (DMM). Earth Planet. Sci. Lett. 231, 53–72.

Figure captions

Figure 1. Simplified geological sketch map of the Lanzo ophiolite in the western Italian Alps after Boudier and Nicolas (1977) and location of the studied area (modified from Sanfilippo et al., 2017)

Figure 2. Field and textural characteristics of the MORB-type dunites. A) Outcrop view of three MORB-type dunite bodies at the Monte Musinè outcrop. B) High temperature foliation in the host Pl-peridotites. C) Detail of a MORB-type dunite showing elongated spinel-trails. E) Irregular clinopyroxene vein intruding a MORB-type dunite.

Figure 3. Field and textural features of the depleted replacive harzburgites. A) Contact zone between depleted replacive harzburgites and deformed Pl-peridotites. Relicts of the high temperature foliation are still visible. B) Irregular clinopyroxene-rich vein crosscutting a depleted replacive harzburgite. C) Interstitial clinopyroxene (Cpx) and Cr-spinel (Spl) in backscattered image.

Figure 4. a) Variability in spinel Mg/(Mg+Fe) (mol%) versus Cr/(Cr+Al) (mol%) of Lanzo South replacive bodies and host peridotites compared to abyssal peridotites (data from Warren, 2012; Sani et al., 2020). Also indicated are melting and melt-rock reaction trends starting from Depleted MORB Mantle (DMM) compositions (see Workman and Hart, 2005). b-c) Chondrite-normalized trace element compositions of olivine and clinopyroxene from the Lanzo South replacive bodies compared to lower crustal gabbros from Alpine-Apennine ophiolites and host harzburgites (data from Sanfilippo et al., 2014). Detection limits of olivine compositions are also indicated with dashed grey line. d) Whole rock covariations between Al_2O_3 (wt%) and MgO (wt%), Os (ppb) and Re (ppb) contents in Lanzo South replacive bodies and host Pl-peridotites. The dashed line indicates correlations for the depleted harzburgites.

Figure 5. Initial (at 160 Ma) Nd-Hf isotope compositions of clinopyroxene separates from the replacive bodies of Lanzo South and host Pl-peridotites compared to whole rock compositions of Lanzo North peridotites (Guarnieri et al., 2010) and Alpine-Apennine ophiolite MORB (compiled from Rampone and Sanfilippo, 2021). Also shown are the clinopyroxene Nd-Hf isotope compositions of present-day oceanic mantle peridotites (Stracke et al., 2011; Sani et al., 2022) and Atlantic MORB glasses.

Figure 6. Chondrite-normalised platinum-group element concentrations for Lanzo South Pl-peridotites (a), depleted harzburgites (b) and MORB-type dunites (c) (CI chondrite values from Horan et al., 2003) compared to the compositions of abyssal peridotites (see Snow and Reisberg 1995; Luguet et al. 2001; 2003; Harvey et al., 2006; 2011; Liu et al., 2009; Marchesi et al., 2014; Lassiter et al., 2014; Day et al., 2017), cratonic peridotites (from Becker et al., 2006) and replacive dunites (Rehkamper et al. 1999; Buchl et al., 2004; Standish et al., 2002; Harvey et al., 2011; Marchesi et al., 2014). Olivine-rich troctolites and dunites from the crust-mantle boundary exposed at the Uraniwa Hills, Central Indian Ridge (Sanfilippo et al., 2016), are also shown.

Figure 7. Bulk rock Al_2O_3 versus (a) $^{187}Os/^{188}Os$, (b) $^{187}Re/^{188}Os$ and (c) Ir/Pd ratios of Lanzo South replacive bodies and host Pl-peridotites. Also shown are peridotites from Lanzo North (Lorand et al., 2000; Becker et al., 2006). Primitive Upper Mantle values from Becker et al. (2006)

Figure 8. Bulk rock $^{187}Os/^{188}OS$ versus clinopyroxene eHf (initial values at 160 Ma) of Lanzo South replacive bodies and host Pl-peridotites. Also indicated are abyssal peridotites (data from Martin et al., 1991; Snow and Reisberg; 1995; Liu et al, 2008; Stracke et al., 2011; Day et al., 2017). Note that ancient melting would produce inverse correlations in Os versus Hf isotope ratios as a consequence of radiogenic Os and Hf ingrowth, as displayed by the refractory peridotites from Gakkel Ridge (see Liu et al., 2008; Stracke et al., 2011).

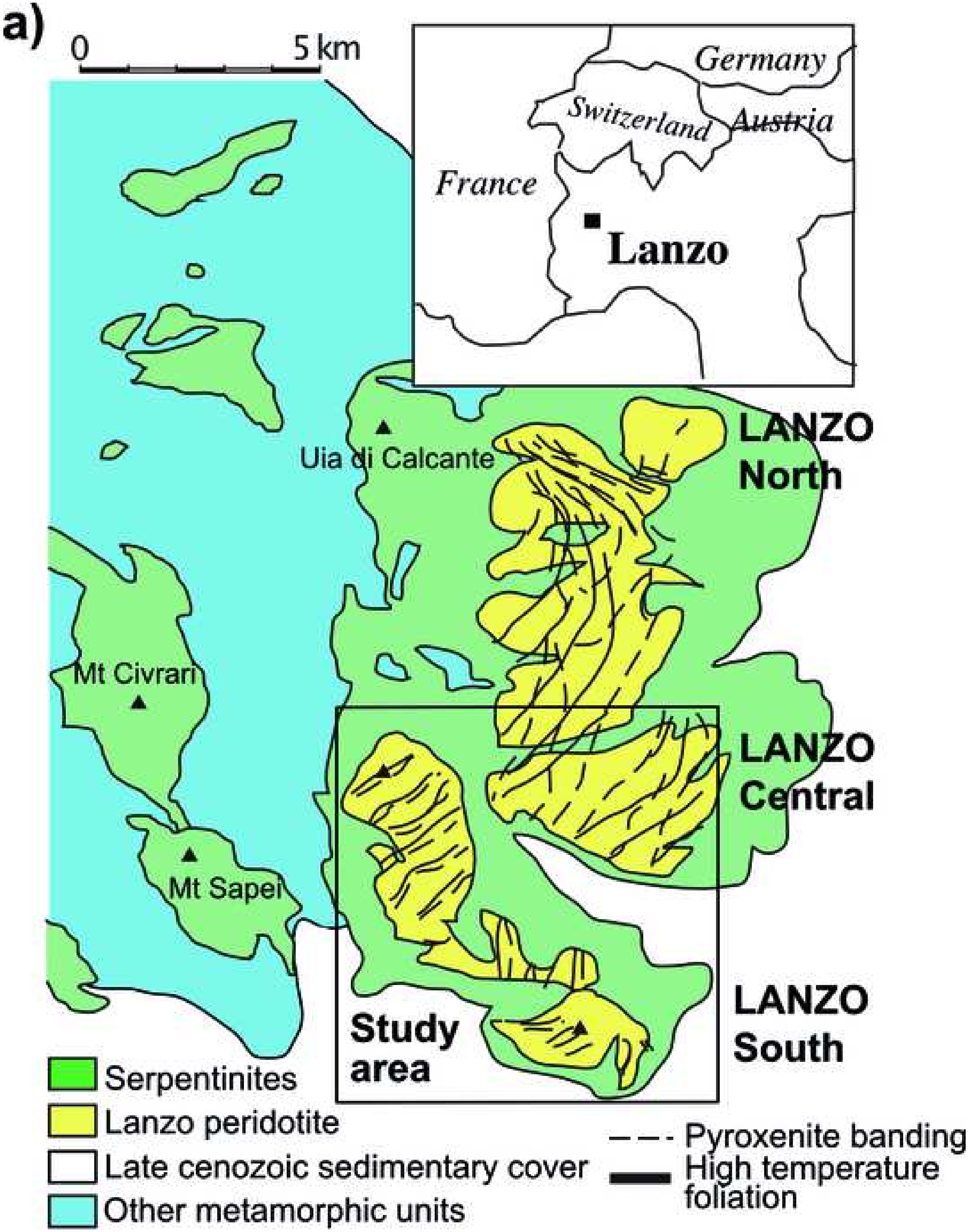
a)
0
5 km
Germany
Switzerland
Austria
France
Lanzo
LANZO North
Uia di Calcante
Mt Civrari
Mt Sapei
LANZO Central
LANZO South
Study area
Serpentinites
Lanzo peridotite
Late cenozoic sedimentary cover
Other metamorphic units
Pyroxenite banding
High temperature foliation

Figure 2

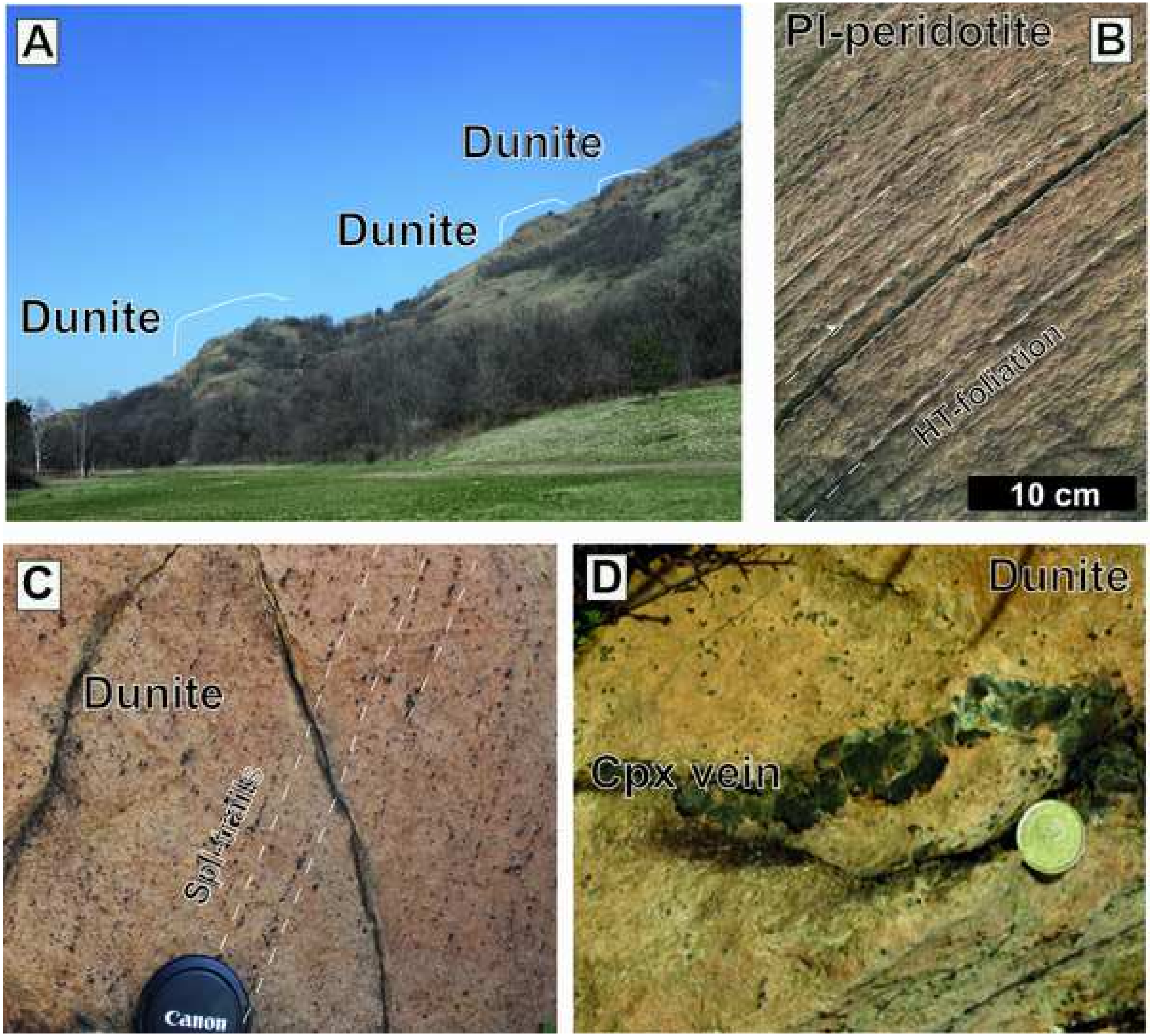
A
Dunite
Dunite
Dunite
Pl-peridotite
B
HT-foliation
10 cm
C
Dunite
Spl-trails
Canon
D
Dunite
Cpx vein

Figure 3

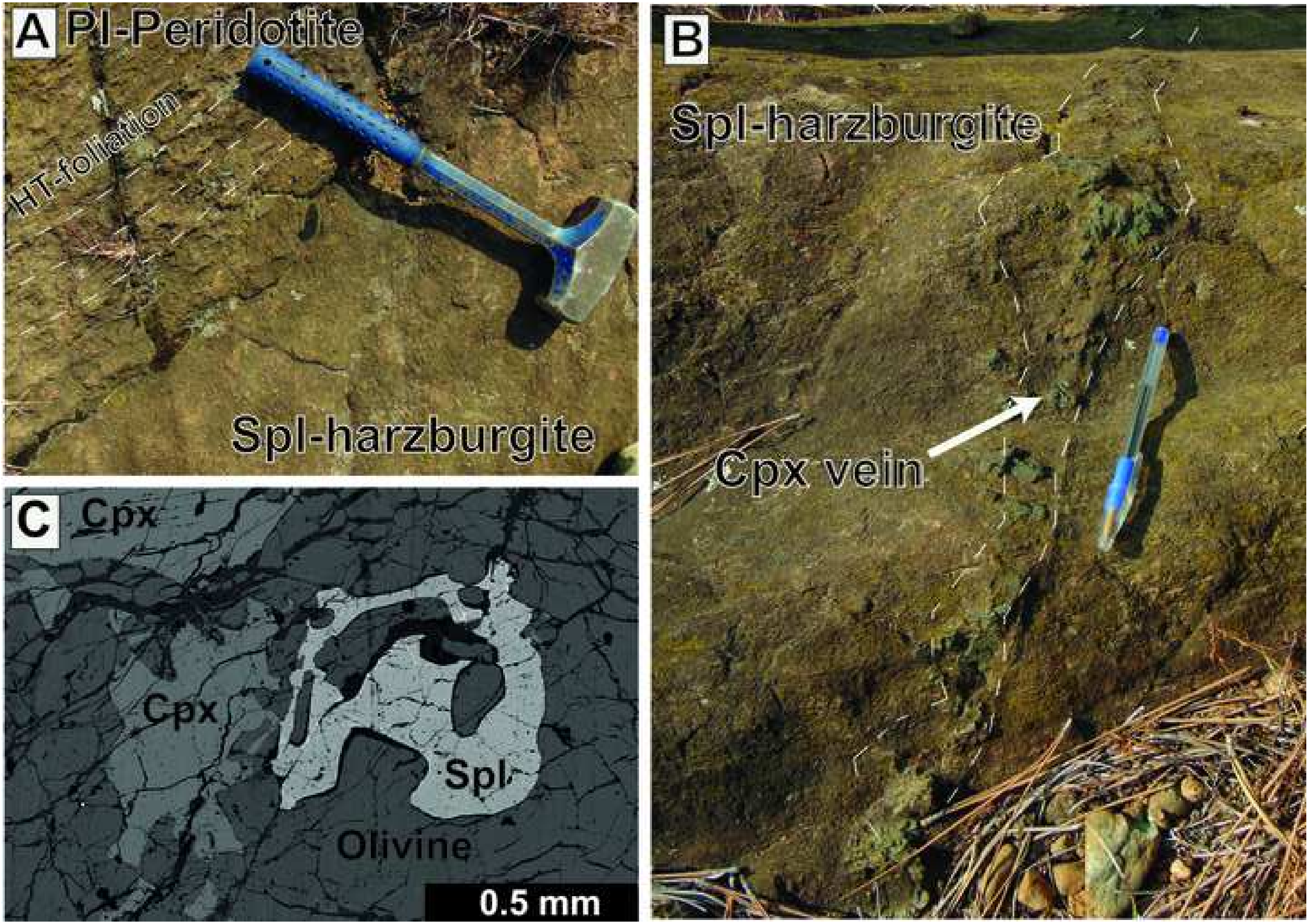
A
Pl-Peridotite
HT-foliation
Spl-harzburgite
B
Spl-harzburgite
Cpx vein
C
Cpx
Cpx
Spl
Olivine
0.5 mm

Figure 4

Click here to access/download;Figure;Fig.4.jpg

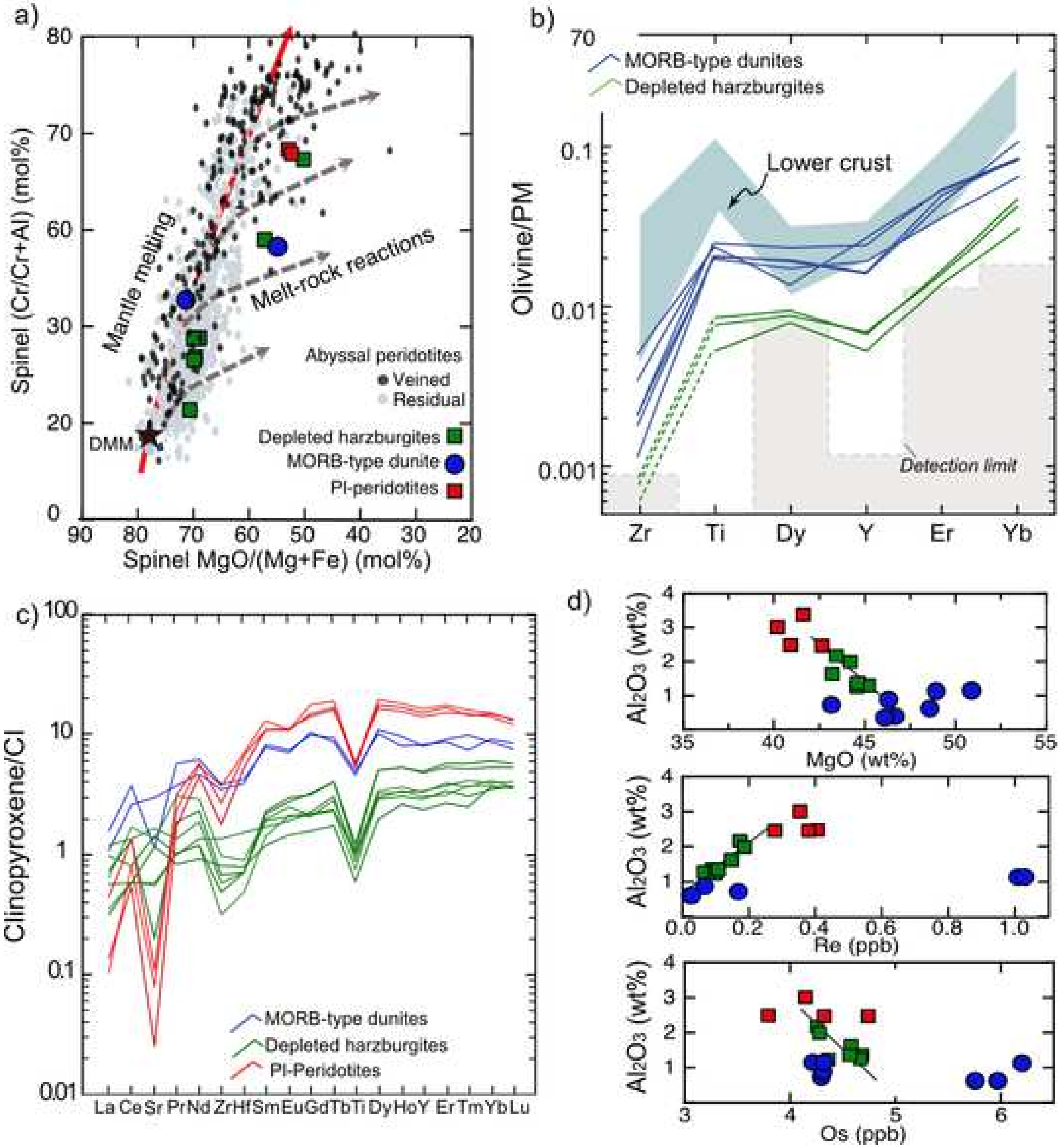

Figure 5

Click here to access/download;Figure;Fig.5.jpg

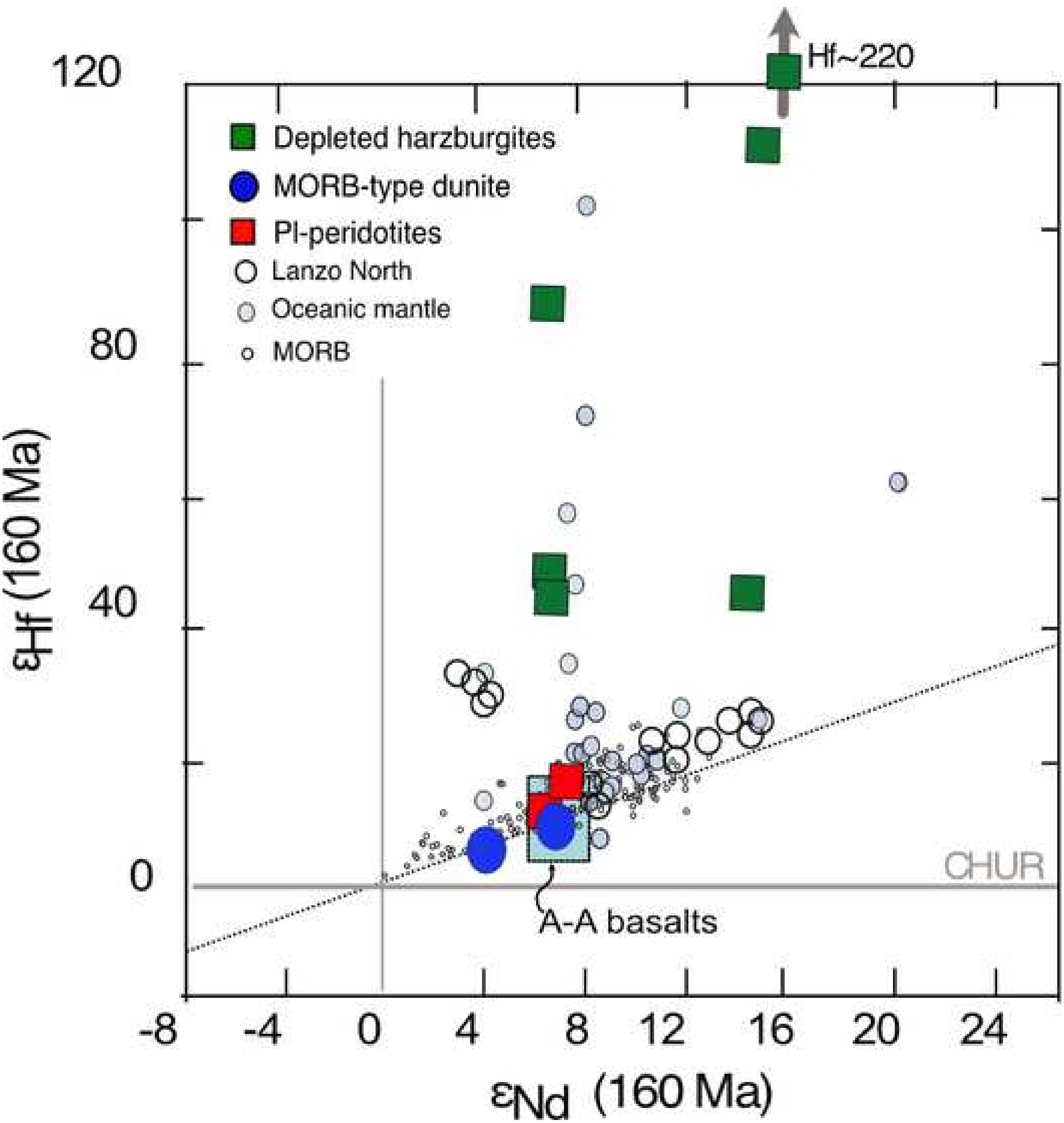

Figure 6

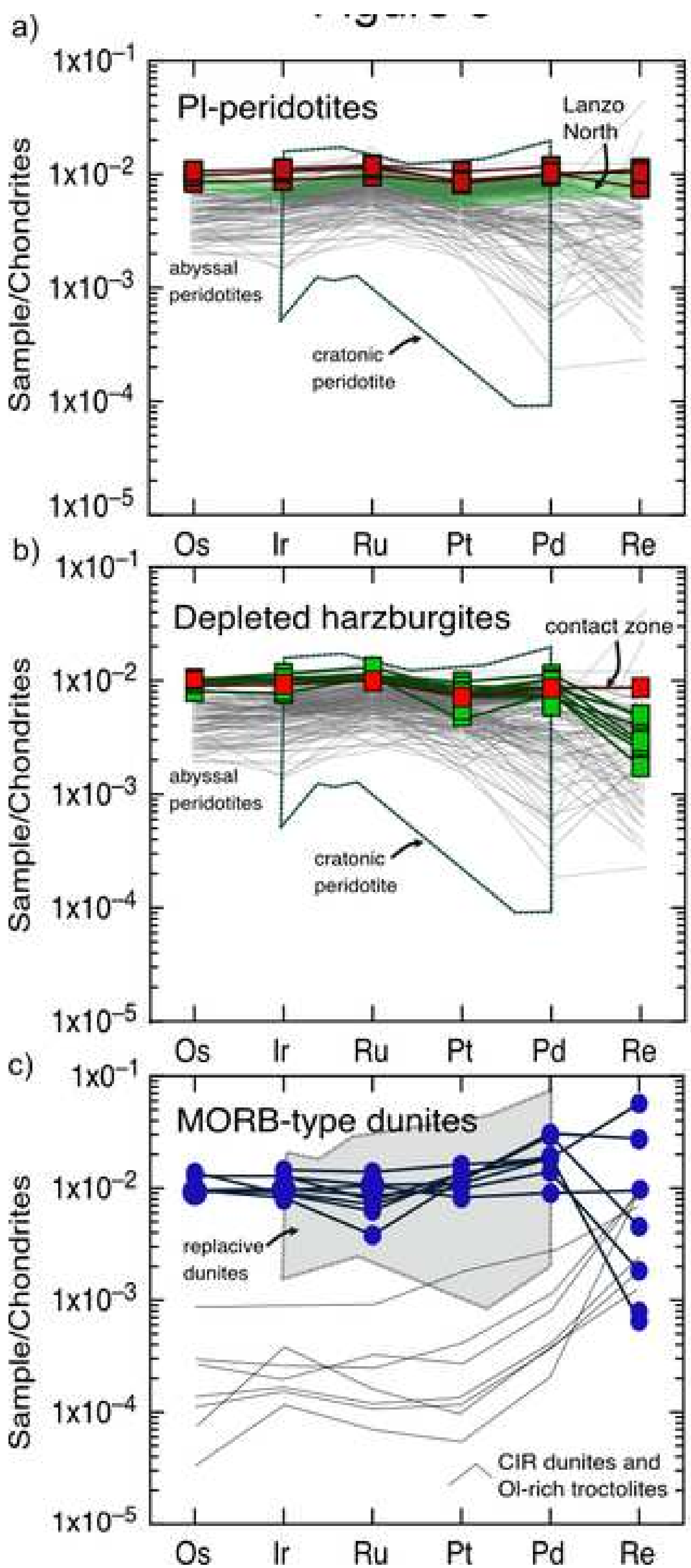
a)
Pl-peridotites
Lanzo North
abyssal peridotites
cratonic peridotite
Sample/Chondrites
1x10⁻¹
1x10⁻²
1x10⁻³
1x10⁻⁴
1x10⁻⁵
Os
Ir
Ru
Pt
Pd
Re
b)
Depleted harzburgites
contact zone
abyssal peridotites
cratonic peridotite
Sample/Chondrites
1x10⁻¹
1x10⁻²
1x10⁻³
1x10⁻⁴
1x10⁻⁵
Os
Ir
Ru
Pt
Pd
Re
c)
MORB-type dunites
replacive dunites
CIR dunites and Ol-rich troctolites
Sample/Chondrites
1x0⁻¹
1x10⁻²
1x10⁻³
1x10⁻⁴
1x10⁻⁵
Os
Ir
Ru
Pt
Pd
Re

Figure 7

Click here to access/download;Figure;Fig.7.jpg

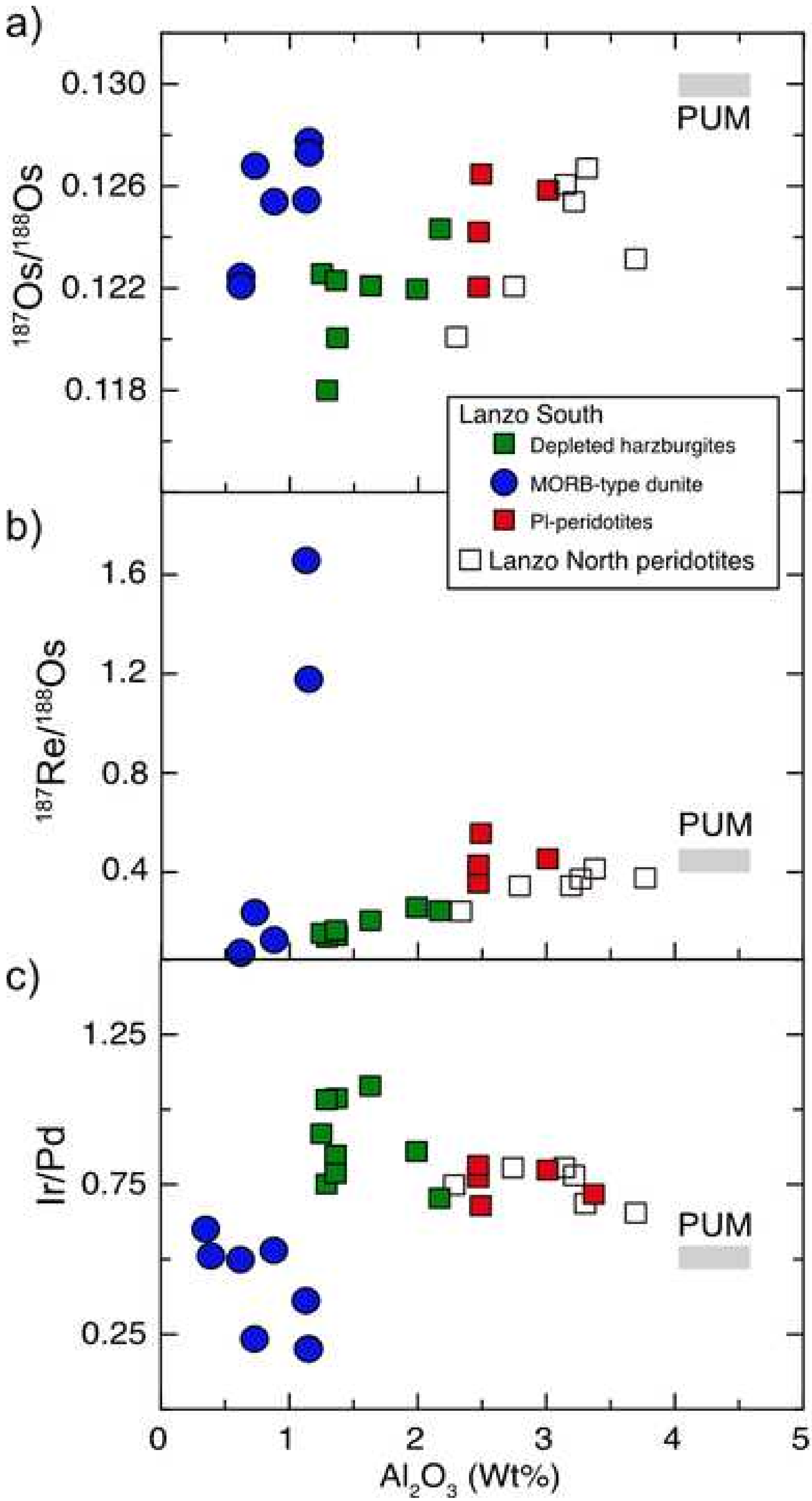

Figure 8

Click here to access/download;Figure;Fig.8.jpg

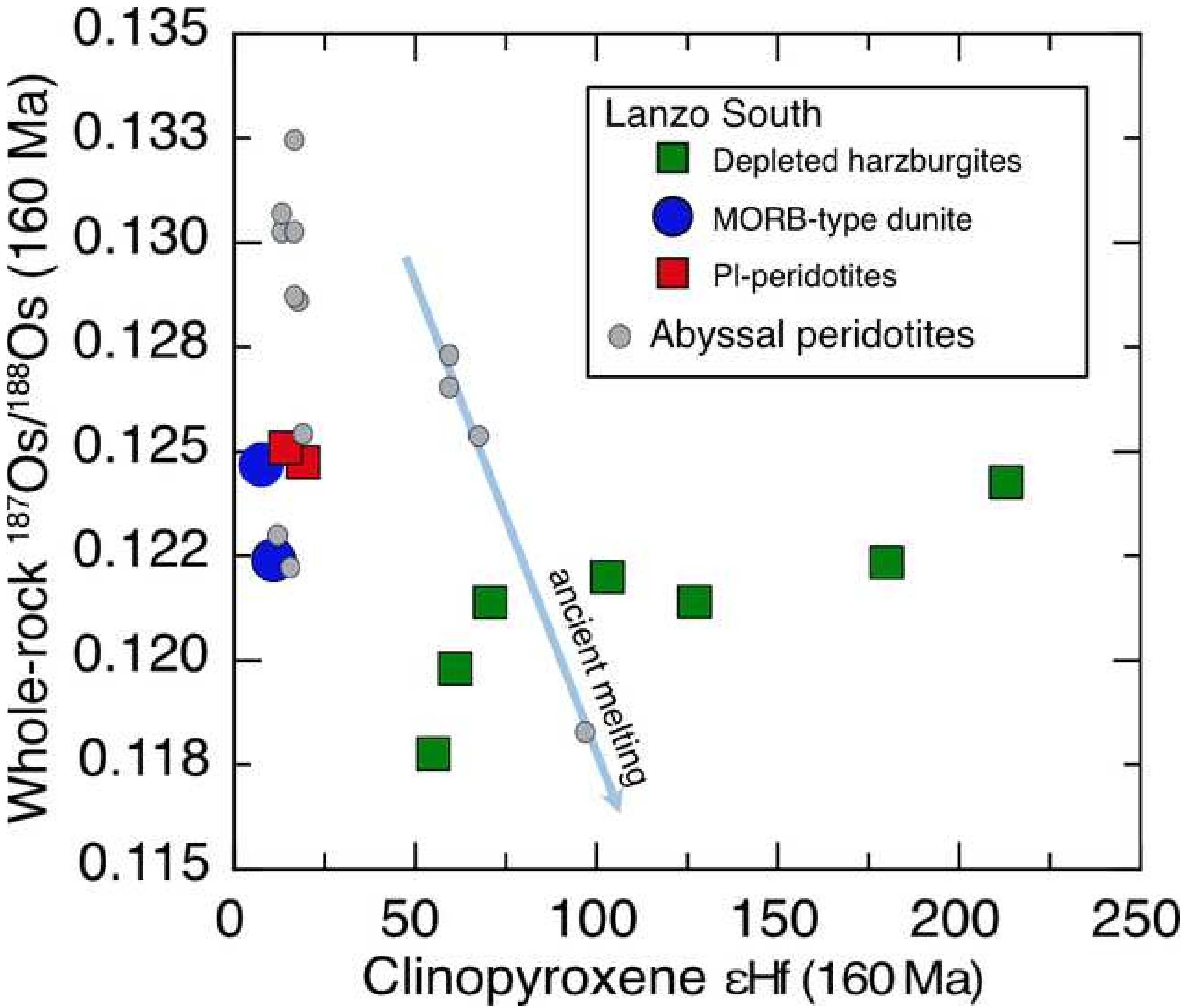

Supplementary file table

Click here to access/download
Supplementary file
TableSupplementary_SAnfilippo et al., ReplLanzo.xlsx

Declaration of interests

☒The authors declare that they have no known competing financial interests or personal relationships that could have appeared to influence the work reported in this paper.

☐The authors declare the following financial interests/personal relationships which may be considered as potential competing interests: